J|A|C|S
COMMUNICATIONS

Published on Web 05/29/2002

Quantum Dynamics of Hydride Transfer Catalyzed by Bimetallic Electrophilic Catalysis: Synchronous Motion of Mg^{2+} and H^- in Xylose Isomerase

Mireia Garcia-Viloca, Cristóbal Alhambra, Donald G. Truhlar,* and Jiali Gao*

Department of Chemistry and Supercomputer Institute, University of Minnesota, Minneapolis, Minnesota 55455-0431

Received April 1, 2002

The enzyme xylose isomerase (D-xylose ketol-isomerase, EC5.3.1.5) is very important in carbohydrate biotechnology because of its role in the industrial catalysis of the interconversion of aldose and ketose sugars.[1] The enzyme requires divalent metals as a cofactor, and Mg^{2+} plays this role in vivo. The physiological substrate is the pentose D-xylose, which is converted to xylulose; the most important biotechnological substrate is the hexose D-glucose, which is converted to fructose. The enzyme is an important target for protein engineering to change the metal specificity or the pH dependence of activity.[2,3] This enzyme is also very important from a fundamental point of view since it exhibits the widespread and intriguing bridged-bimetallic active-site motif in which the substrate is bound to two metals connected by a glutamate bridge,[4−8] and X-ray crystallographic studies find two positions for one of the metal atoms, which suggests that metal movement is involved in catalysis.[5−8]

Xylose isomerase binds sugars in their closed form and catalyzes the ring opening prior to the chemical step, which has been postulated to occur by hydride transfer promoted by the electrophilic metallic cofactor,[5−12] although proton-transfer mechanisms were also considered in earlier work. Theoretical work involving model compounds[13] and structural[14] and tunneling calculations[15] in energy-optimized structures have elucidated several aspects of the reaction.

A detailed mechanism has been proposed for the isomerization on the basis of isotope exchange studies[16] and X-ray structures.[5,7] The mechanism involves both Mg ions. One of these exhibits an intact coordination shell throughout the process (including coordination to O2 and O4 of the sugar; see Figure 1) and is called the structural Mg (or Mg^s); the other undergoes ligand changes and large-amplitude motion (>1 Å) and is called the catalytic Mg (or Mg^c). After ring opening, a proton is transferred from O2 to an OH on Mg^c, and Mg^c is drawn toward the negatively charged O2 (which then bridges the two Mg). This enables Mg^c to catalyze a rate-limiting[11] hydride shift from C2 to C1. Eventually O1 is protonated, the ring is closed, and product is released.

Here we report classical/quantal dynamical simulations of the xylose isomerization that provide new insight into the metal motion. We obtained a starting geometry for the hydride-transfer reaction corresponding to the mechanism above by prior simulation of the proton-transfer step in which the reaction path was explored by two successive umbrella sampling studies, first employing a reaction coordinate defined as the proton-to-O2 distance minus the proton-to-acceptor distance and then employing the Mg−Mg distance R as the reaction coordinate. Starting with a typical member of the resulting ensemble, it required only changes in torsion angles and side chain orientations to obtain a structure very similar to that postulated by Whitlow et al.[5] for the hydride-transfer step. After minimization and equilibration, the hydride-transfer step was then studied by umbrella sampling with the reaction coordinate defined as the hydride-to-C2 distance minus the hydride-to-C1 distance.

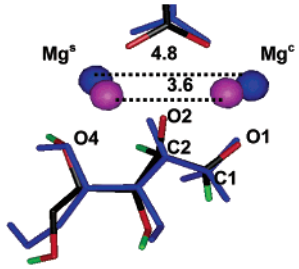

Figure 1. Reactant (black, red, green, and violet) and product (blue) states of the hydride-transfer step. The glutamate-bridged bimetallic prosthetic group is at the top, and xylose is at the bottom. Hydrogen atoms on C3, C4, and C5 are not shown; others are shown in green for the reactant and blue for the product. Distances are in Å.

We treated all 19 atoms of xylose (with O2 deprotonated) by quantum mechanics (QM) with semiempirical molecular orbital theory with parameters from PM3[17] and the rest of the system by molecular mechanics (MM) with the parameters of the CHARMM[18] and TIP3P[19] force fields. The QM and MM parts are coupled by nonbonded electrostatic and van der Waals interactions.[20] The final potential includes a simple valence bond (SVB)[21] potential which was first adjusted to match MP2/6-31+G(d)[22] results for a model hydride-transfer reaction in the gas phase and then further refined on the basis of the experimental[2,3] k_{cat}. The parameters of the SVB potential are given in Supporting Information.

The rate constant for the hydride-transfer step was calculated by ensemble-averaged (EA) dynamical simulations including both variational transition-state theory[23] (VTST) for determination of the statistically averaged dynamical bottleneck and optimized multidimensional tunnneling (OMT) calculations[24−27] for the nonclassical aspects of the chemical step. Ensemble-averaged dynamics is very important for reliable modeling of enzyme mechanisms in general and is particularly important for the present reaction because of the metal-atom movement that accompanies catalysis. First we used umbrella sampling[28] on a 25317-atom system surrounded by stochastic boundary conditions[29] on a 24 Å sphere to calculate a classical mechanical potential of mean force[26,30] (PMF) along the reaction coordinate z, defined as the hydride-to-C2 distance minus the hydride-to-C1 distance. Then we added quantized vibrational free energy[31] in 89 active-site degrees of freedom orthogonal to z to yield a quantized free energy of activation profile, the maximum of which ($\Delta G^{\ddagger}$) identifies the first-stage variational transition state (VTS) at $z = z*$. We then selected five configurations i from the ensemble with $z = z* \pm 0.05$ Å to calculate ensemble-averaged transmission coefficients[32,33]

$$\gamma = \langle \kappa_i \Gamma_i \rangle \qquad (1)$$

* To whom correspondence should be addressed. E-mail: truhlar@umn.edu and gao@chem.umn.edu.

10.1021/ja026383d CCC: $22.00

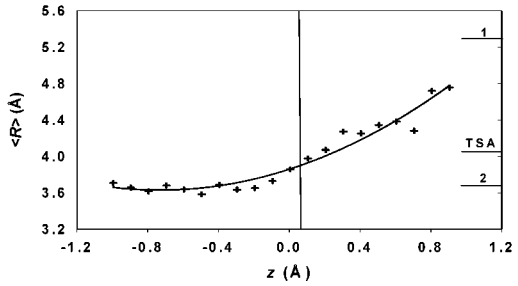

Figure 2. Average Mg−Mg distance, $\langle R \rangle$, as a function of the reaction coordinate, *z*, for the hydride-transfer step. Each point represents the average of *R* in an interval of width 0.1 Å. The vertical line shows the position of the VTS. The horizontal lines denote the values of $\langle R \rangle$ for positions 1 and 2 of the Mg^c in the X-ray structure with glucose and the value of $\langle R \rangle$ for the X-ray structure of the transition-state analogue (TSA).

where Γ_i accounts for recrossing the first-stage VTS, and κ_i accounts for tunneling and nonclassical reflection. The transmission coefficients were calculated in the static secondary zone approximation[33] with 32 atoms in the primary zone. The recrossing correction is computed by VTST using the minimum-energy path[23] for ensemble member *i*, and the tunneling contributions are calculated by the microcanonical OMT method,[25] which involves comparing the small-curvature tunneling approximation[24] to the large-curvature[27] one; the former gives more tunneling.

Our simulations show that the average Mg−Mg distance, $\langle R \rangle$, increases monotonically as a function of *z*. As shown in Figure 2, the average Mg−Mg distance increases from 3.6 Å at the reactant value of *z* to 3.9 Å at $z* = 0.045$ Å, which is the location of the VTS, and then increases dramatically as the system progresses toward products. The range of $\langle R \rangle$ along the reaction path is consistent with the values of $\langle R \rangle$ corresponding to the two positions (labeled[7] 1 and 2) of Mg^c in the X-ray structure[7] with glucose, thus providing a dynamical demonstration of the postulated role[5,7,14] of these two sites in catalysis. As illustrated in Figure 1, *R* is relatively small in the reactant state, and Mg^c is close to O2 (2.01 Å). Dynamical fluctuation of the Mg^c ion modulates charge migration between O2 and O1. As *R* increases and the Mg^c−O2 distance elongates, the C1═O1 carbonyl group is more polarized by Mg^c, favoring localization of a negative charge on O1, which in turn promotes the hydride shift from C2 to C1. As this shift proceeds, Mg^c synchronously recedes from Mg^s and from O2 (the average Mg^c-to-O2 distance is 2.10 Å at the VTS and 3.46 Å at the product, at which a water molecule has replaced O2 in the coordination shell of Mg^c). Figure 2 also shows the X-ray value[8] of $\langle R \rangle$ when xylose isomerase is cocrystallized with the transition-state analogue, D-threonohydroxamic acid. This value is encouragingly close to the value we find at the VTS.[34]

The model is validated by calculating the primary kinetic isotope effect (KIE) for the chemical step, that is, the ratio of the rate constant for hydride transfer to that for deuteride transfer. Enzymatic KIEs are the best source of information about the extent and nature of bond rearrangement at the transition state. Measured KIEs for the D-glucose substrate range from 2.7 to 4.0 at 333−338 K.[2,3,10] These measurements on $C_6H_{11}DO_6$ may be compared to our calculation on $C_5H_9DO_5$ because the kinetics are very similar for glucose and xylose.[2] van Bastelaere et al.[3] found a KIE of 2.7 for Mg^{2+} cofactor and suggested that if the hydride shift were fully rate-limiting, it could be even larger since they found 3.4 with Mn^{2+}. Furthermore the KIE is expected to decrease with temperature. We calculated a xylose KIE of 3.8 at 298 K, which is consistent with the experiments. More than half of our KIE is due to tunneling; neglecting quantum effects on the reaction coordinate reduces the calculated KIE to 1.8.[35]

Acknowledgment. This work was supported in part by the NSF under Grant No. CHE00-92019 and the NIH. We thank the Fulbright Scholar Program and the Generalitat de Catalunya for an award of a Fulbright Visiting Scholarship to M.G.-V.

Supporting Information Available: Parameters and mathematical expression of the SVB potential (PDF). This material is available free of charge via the Internet at http://pubs.acs.org.

References

(1) Bhosale, S. H.; Rao, M. B.; Deshpande, V. V. *Microbiol. Rev.* **1996**, *60*, 280.
(2) van Tilbeurgh, H.; Jenkins, J.; Chiadmi, M.; Janin, J.; Wodak, S. J.; Mrabet, N. T.; Lambeir, A.-M. *Biochemistry* **1992**, *31*, 5467.
(3) van Bastelaere, P. B. M.; Kersters-Hilderson, L. M.; Lambeir, A.-M. *Biochem. J.* **1995**, *307*, 135.
(4) Carrell, H. L.; Rubin, B. H.; Hurley, T. J.; Glusker, J. P. *J. Biol. Chem.* **1984**, *259*, 3230.
(5) Whitlow, M.; Howard, A. J.; Finzel, B. C.; Poulos, T. L.; Winborne, E.; Gilliland, G. L. *Proteins* **1991**, *9*, 153.
(6) Jenkins, J.; Janin, F.; Rey, F.; Chiadmi, M.; van Tilbeurgh, H.; Lasters, I.; De Maeyer, M.; van Belle, D.; Wodak, S. J.; Lauwereys, M.; Stanssens, P.; Mrabet, N. T.; Snauwert, J.; Matthyssens, G.; Lambeir, A.-M. *Biochemistry* **1992**, *31*, 5449.
(7) Lavie, A.; Allen, K. N.; Petsko, G. A.; Ringe, D. *Biochemistry* **1994**, *33*, 5469.
(8) Allen, K. N.; Lavie, A.; Petsko, G. A.; Ringe, D. *Biochemistry* **1995**, *34*, 3742.
(9) Ramchander, S.; Feather, M. S. *Arch. Biochem. Biophys.* **1977**, *178*, 576. Farber, K. G.; Glasfeld, K. G.; Tiraby, G.; Ringe, D.; Petsko, G. A. *Biochemistry* **1989**, *28*, 7289. Collyer, C. A.; Hendrick, K.; Blow, D. M. *J. Mol. Biol.* **1990**, *212*, 211.
(10) Lee, C.; Bagdasarian, M.; Meng, M.; Zeikus, J. G. *J. Biol. Chem.* **1990**, *265*, 19082.
(11) Rangarajan, M.; Hartley, B. S. *Biochem. J.* **1992**, *283*, 223.
(12) Nagorski, R. W.; Richards, J. P. *J. Am. Chem. Soc.* **1996**, *118*, 7432.
(13) Zheng, Y.-J.; Merz, K. M. Jr.; Farber, G. K. *Protein Eng.* **1993**, *6*, 479. Fuxreiter, M.; Farkas, O.; Naray-Szabo, G. *Protein Eng.* **1995**, *8*, 925. Ferenczy, G.; Naray-Szabo, G.; Varnai, P. *Int. J. Quantum Chem.* **1999**, *75*, 215.
(14) Hu, H.; Liu, H.; Shi, Y. *Proteins* **1997**, *27*, 545.
(15) Nicoll, R. M.; Hindle, S. A.; MacKenzie, G.; Hillier, I. H.; Burton, N. A. *Theor. Chem. Acc.* **2001**, *106*, 105.
(16) Allen, K. N.; Lavie, A.; Farber, G. K.; Glasfeld, A.; Petsko, G. A.; Ringe, D. *Biochemistry* **1994**, *33*, 1481.
(17) Stewart, J. J. P. *J. Comput. Chem.* **1989**, *10*, 221.
(18) MacKerell, A. D., Jr.; Bashford, D.; Bellott, M.; Dunbrack, R. L., Jr.; Evanseck, J. D.; Field, M. J.; Fischer, S.; Gao, J.; Guo, H.; Ha, S.; Joseph-McCarthy, D.; Kuchnir, L.; Kuczera, K.; Lau, F. T. K.; Mattos, C.; Michnick, S.; Ngo, T.; Nguyen, D. T.; Prodhom, B.; Reiher, W. E., III; Roux, B.; Schlenkrich, M.; Smith, J. C.; Stote, R.; Straub, J.; Watanabe, M.; Wiorkiewicz-Kuczera, J.; Yin, D.; Karplus, M. *J. Phys. Chem. B* **1998**, *102*, 3586.
(19) Jorgensen, W. L.; Chadrasekhar, J.; Madura, J. D.; Impey, R. W.; Klein, M. L. *J. Chem. Phys.* **1983**, *79*, 926.
(20) Field, M. J.; Bash, P. A.; Karplus, M. *J. Comput. Chem.* **1990**, *11*, 700.
(21) Devi-Kesavan, L. S.; Garcia-Viloca, M.; Gao, J. *Theor. Chem. Acc.* **2002**, submitted.
(22) Hehre, W. J.; Radom, L.; Schleyer, P. v. R.; Pople, J. A. *Ab Initio Molecular Orbital Theory*; Wiley: New York, 1986.
(23) Truhlar, D. G.; Garrett, B. C. *Acc. Chem. Res.* **1980**, *13*, 440. Truhlar, D. G.; Garrett B. C. *Annu. Rev. Phys. Chem.* **1984**, *35*, 159.
(24) Liu, Y.-P.; Lynch, G. C.; Truong, T. N.; Lu, D.-h.; Truhlar, D. G.; Garrett, B. C. *J. Am. Chem. Soc.* **1993**, *115*, 2408.
(25) Liu, Y.-P.; D.-h. Lu, Gonzàlez-Lafont, A.; Truhlar, D. G.; Garrett, B. C. *J. Am. Chem. Soc.* **1993**, *115*, 7806.
(26) Truhlar, D. G.; Liu, Y.-P.; Schenter, G. K.; Garrett, B. C. *J. Phys. Chem.* **1994**, *98*, 8396.
(27) Fernandez-Ramos, A.; Truhlar, D. G. *J. Chem. Phys.* **2001**, *114*, 1491.
(28) Kottalam, J.; Case, D. A. *J. Am. Chem. Soc.* **1988**, *110*, 7690.
(29) Brooks, C. L., III; Brünger, A.; Karplus, M. *Biopolymers* **1985**, *24*, 843.
(30) Case, D. A.; McCammon, J. A. *Ann. N.Y. Acad. Sci.* **1986**, *482*, 222. Fonseca, T. In *The Enzyme Catalysis Process*; Cooper, A., Houben, J. L., Chien, L. C., Eds.; NATO Advanced Study Institute Series A 178; Plenum: New York, 1988; p 331. Gao, J. *J. Am. Chem. Soc.* **1993**, *115*, 2930. Gao, J.; Truhlar, D. G. *Annu Rev. Phys. Chem.* **2002**, *53*, 467.
(31) Garcia-Viloca, M.; Alhambra, C.; Truhlar, D. G.; Gao, J. *J. Chem. Phys.* **2001**, *114*, 9953.
(32) Anderson, J. B. *Adv. Chem. Phys.* **1995**, *91*, 381.
(33) Alhambra, C.; Corchado, J.; Sánchez, M. L.; Garcia-Viloca, M.; Gao, J.; Truhlar, D. G. *J. Phys. Chem. B* **2001**, *105*, 11326. Truhlar, D. G.; Gao, J.; Alhambra, C.; Garcia-Viloca, M.; Corchado, J.; Sánchez, M. L.; Villà, J. *Acc. Chem. Res.* **2002**. In press.
(34) The average Mg^c−O1 distance is 2.08, 1.95, and 1.89 Å, at the reactant, transition state, and product.
(35) For H(D), we find $\Delta G^{\ddagger} = 23.7(24.1)$ kcal/mol, $\langle \kappa_i \rangle = 6.9(3.3)$, and $\langle \Gamma_i \rangle = 0.95(0.95)$.

JA026383D